

www.pharmaerudition.org

ISSN: 2249-3875



International Journal of Pharmaceutical Erudition

Research for Present and Next Generation

Aug. 2015

Vol: 05 Issue: 02

(9-17)





Research Paper

Study on the Ultrasonic-assistant Electro-catalytic Oxidation of Salicylic Acid in Water

Bin Mei ^a, Xiaolong Zhang ^b, Qian Ma ^{c*}

^a Shanghai University of Medicine & Health Sciences, Shanghai, China

^b Environmental Engineering, University of Connecticut, Connecticut, USA

^c Environmental Protection Bureau in Hongkou District, Shanghai, China

The electrocatalytic oxidation and ultrasonic-assistant electrocatalytic oxidation were used respectively to the degradation of salicylic acid. Through the UV spectra it was proved some ultraviolet-absorbent intermediates were formed during the degradation. The peak absorbance varied with lapse of time, and the relationships were fitted by NLSF. The results showed that the reductions of relative peak absorbance both met the pseudo first-order reaction kinetics in two processes. The existence of $\cdot\text{OH}$ was assayed by cyt-c (II) colorimetry and addition of mannitol. The intermediates formic acid, acetic acid and phenol were detected by GC-MS after degradation for 60 min. A general reaction pathway that accounted for salicylic acid degradation to CO_2 and water involving those intermediates was proposed.

Keywords: electrocatalytic oxidation, ultrasonic, salicylic acid, hydroxyl radical, mechanism.

INTRODUCTION

Salicylic acid (SA), also called orthohydroxy benzoic acid, is easy to sublime and volatilize with vapor, and has the character of phenol and carboxylic acid.¹

The water containing high concentration of SA can seriously affect human's health.² although the biochemical process is a popular method in treating organic pollutions,³⁻⁹ SA is biologically refractory, resulting in huge energy consumption and low efficiency.¹⁰

Since SA is biologically refractory, the biochemical processes are not effective in treating SA due to Thus the non-biochemical processes have been developed.

For example, SA can be thoroughly degraded by $\text{UV}/\text{H}_2\text{O}_2/\text{O}_2$ process.¹¹ Light catalytic oxidation is widely used at present, especially TiO_2 which has good catalytic activity for SA.¹² Electrocatalytic oxidation is a promising method that has been used to treat many types of organics.¹³⁻¹⁶ The

electrocatalytically active electrodes can produce oxidants such as $\cdot\text{OH}$, O_3 , and H_2O_2 , by which the organic substances can be degraded.¹⁷ However, the practical applications of electrocatalytic oxidation in treating SA containing water are limited by the low oxygen evolution potential and high cost.¹⁸ Meanwhile, the improvement of the structures of electrode and electrolytic reactor are needed for decreasing the energy consumption.¹⁹

Ultrasonic can produce cavitation bubbles with high temperature and pressure which can facilitate energy and mass transfer, decomposition of reactants, formation of radicals, homogenous and heterogenous reactions.²⁰ Single ultrasonic oxidation needs more energy to treat organic substances but results in worse efficiency, so current researches focus on the combination of ultrasonic and other technologies.²¹⁻²³ Electrochemistry combined with ultrasonic, called

sono electrochemistry, shows many advantages, including continuous rinse and activation to the surface of electrode, elimination of the bubble accumulation on the surface and great increase of mass transfer rate.²⁴⁻²⁶ Few researches on the combination of electrocatalytic oxidation and ultrasonic have been reported.^{27,28}

In this study, ultrasonic-assistant electrocatalytic oxidation was studied to degrade SA in water and the pathway of SA degradation was also explored. To our knowledge, this research has not been reported yet.

1 Experimental

1.1 Chemicals

Salicylic acid, sodium sulfate, sulfuric acid and sodium hydroxide used in experiments were all analytical grade.

1.2 Experimental method

1.2.1 Preparation of Ti/SnO₂+Sb₂O₃+PtO anode

The meshy titanium was first decreased by 20% hot NaOH solution, and then immersed in a boiling oxalic acid aqueous solution (15%, w/w) for 30 minutes until the oxides were removed. The treated surface was washed by ultra-pure water and stored in absolute ethanol for further treatment.

A layer of conducting oxides was deposited on meshy titanium substrate by thermal treatment. A non-aqueous solution was prepared by successively dissolving SnCl₄·5H₂O, SbCl₃ and H₂PtCl₆ in a mixture of 5.0 ml hydrochloric acid, 20 ml isopropanol and 275 ml ethanol. This solution was brushed onto the titanium base and the solvent was subsequently evaporated at 80 °C for 20 minutes. The pretreated electrode underwent a thermal decomposition in a

muffle furnace at 450 °C for 15 minutes in air atmosphere and then cooled down to room temperature. This procedure (painting, evaporation and thermal treatment) was repeated 10 times. Finally, the electrode was annealed at 600 °C for one hour for stabilization. The average mass density of conducting oxides film was about 1.1 mg·cm⁻², composed of SnO₂, Sb₂O₃ (the molar ratio of Sn to Sb was 6.5 to 1) and PtO in minute quantity.

1.2.2 Experimental equipment

200 ml of SA sample was degraded respectively by electrocatalytic oxidation (ECO) and ultrasonic-assistant electrocatalytic oxidation (USECO) in the electrochemical reactor showed in Fig. 1. 2.0 ml of treated SA were periodically sampled to determine pH and COD_{Cr}.

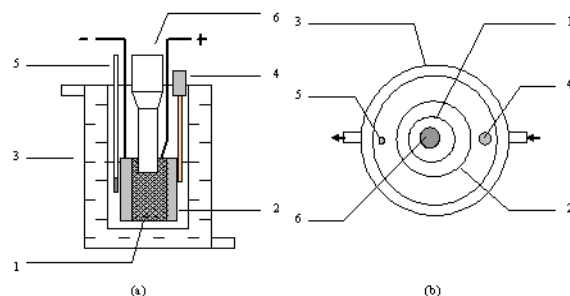


Fig.1 Experimental equipment for ultrasonic-assistant catalytic electrolysis (1: reticulate SnO₂/Sb₂O₃/Ti anode; 2: Ti cathode; 3: cooling jacket; 4: pH meter; 5: thermometer; 6: ultrasonic head)

1.3 Analytical method

1.3.1 pH and COD_{Cr} determination

The solution pH was measured with a PHS-3C pH-meter. COD_{Cr} was determined on HACH DR/2010 COD analyzer.

1.3.2 UV-Vis analysis

UV-Vis analysis was carried on Lambda Bio 40 UV spectrograph (PE). 2 ml of sample was withdrawn by pipette and added into volumetric flask with 10 ml



capacity. 2 ml of NaOH ($10^{-2} \text{ mol}\cdot\text{l}^{-1}$) was also added into flask. This mixture was diluted to the graduation and pH was about 10.3. UV-Vis spectrograph scanned in the range of $\approx 200\text{--}400 \text{ nm}$ with rate of $6 \text{ nm}\cdot\text{s}^{-1}$ where 2 ml of Na_2SO_4 ($10.0 \text{ g}\cdot\text{l}^{-1}$) was treated as blank.

1.3.3 ·OH detection

OH is a substance with high activity, low concentration and short life. Its life in aqueous solution is only 10^{-6} s so that the direct detection is extremely difficult. ESR, HPLC, chemiluminescence and spectrophotometry are widely used in the ·OH detection. The principle of these methods is that ·OH is converted into stable adduct with longer life by ·OH capture agent, which is easier to indirectly detect.

(a) Light red reductive cytochrome c [cyt-c (II)] can be converted into light yellow oxidative state by ·OH. So ·OH content can be determined through the change of reductive cyt-c (II) content by colorimetry. This method is generally used to detect ·OH in the biological system due to easy operation and good specificity. ·OH detection in USECO was made by cyt-c (II) colorimetry.

100 ml of sample, which comprised cyt-c (II) (AR, $M=12384 \text{ g}\cdot\text{mol}^{-1}$, Sigma, $40.4 \text{ mol}\cdot\text{l}^{-1}$), potassium dihydrogenphosphate buffer ($0.15 \text{ mol}\cdot\text{l}^{-1}$, $\text{pH}=7.4$) and Na_2SO_4 ($10 \text{ g}\cdot\text{l}^{-1}$), was degraded by ultrasonic, ECO and USECO for 30 min, respectively. The current intensity was $5 \text{ mA}\cdot\text{cm}^2$ and ultrasonic intensity was $27.1 \text{ W}\cdot\text{cm}^2$. The system gradually turned light red into light yellow. Untreated and treated sample were withdrawn to make UV-Vis analysis in the range of $\approx 350\text{--}600 \text{ nm}$.

(b) Mannitol is widely used as ·OH scavenger in radiation chemistry and biochemistry, so the degradation rate of organic substances must be slower in the presence of mannitol due to the elimination of ·OH. SA was degraded by USECO under the present of mannitol. The impact of mannitol with different concentration on the degradation efficiency was regarded as the assistant detection to prove the ·OH generation during USECO.

1.3.4 GC-MS analysis

200 ml of treated sample was extracted by 50 ml of absolute ethyl ether within 3 times. The solvent was removed by reduced pressure distillation and the extract was concentrated to 0.5 ml. GC-MS analysis was carried on Finnigan Voyager GC-MS apparatus. A HP-INNOWax capillary column ($30 \text{ m} \times 0.25 \text{ mm}$, $0.25 \mu\text{m}$) was used. The temperature program was as follows: $50 \text{ }^\circ\text{C}$ for 2 min, $15 \text{ }^\circ\text{C}\cdot\text{min}^{-1}$ up to $250 \text{ }^\circ\text{C}$, hold for 10 min. Sample volume was $0.5 \mu\text{l}$. Helium was the carrier gas with a $1.0 \text{ ml}\cdot\text{min}^{-1}$ flowrate and a 15: 1 split ratio. The mass detector was operated in the EI mode, scanning in the range of 35–500 amu with a rate of 0.5 sec per time. Ionization voltage was 70 eV and temperature was $200 \text{ }^\circ\text{C}$. Voltage and emit current of enhanced tube were 400 eV and 100 mA. The detection results were compared with NIST standard database.

2 Results and discussion

2.1 ·OH detection in USECO

2.1.1 Cyt-c (II) colorimetry

As Fig. 2 showed, cyt-c (II) had two specific absorption peaks at ≈ 414 and 550 nm ($t=0$). The

absorption curve of sample degraded only by ultrasonic for 30 min was almost same as that of original sample. However, during ECO and USECO after 30 min, the peak at 550 nm disappeared and the peak at 414 nm removed to 404 nm with obvious decrease of peak value. It demonstrated that $\cdot\text{OH}$ generated by 20 kHz ultrasonic was low enough to overlook while it was actually produced during USECO.

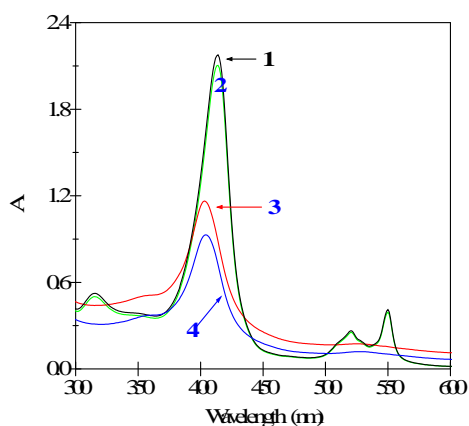


Fig. 2 The UV-Vis adsorption spectra of cytochrome c (II) oxidation

(Curve 1: $t = 0$ min; 2: $t = 30$ min, ultrasonic only; 3: $t = 30$ min, electrocatalytic oxidation; 4: $t = 30$ min, ultrasonic-assistant electrocatalytic oxidation)

Moreover, the decrease of peak value in USECO was bigger than that in ECO. These two degradation methods operated under the same current intensity, reaction time and electrode, thus $\cdot\text{OH}$ yields were surely same ($\cdot\text{OH}$ generated by ultrasonic was overlooked). So it was presumed that the assistance of ultrasonic on electrocatalytic system was to facilitate mass transfer and more cyt-c (II) was oxidized by $\cdot\text{OH}$ accumulated near the surface of electrode.

2.1.2 Addition of mannitol

The initial concentration of SA was $0.96 \text{ mmol}\cdot\text{L}^{-1}$. Other conditions were same as 2.1. The impact of mannitol

with different concentration was depicted in Fig. 3. UV-Vis spectra (Fig. 4) of $5.0 \text{ mmol}\cdot\text{L}^{-1}$ mannitol before (a) and after (b) USECO for 60 min.

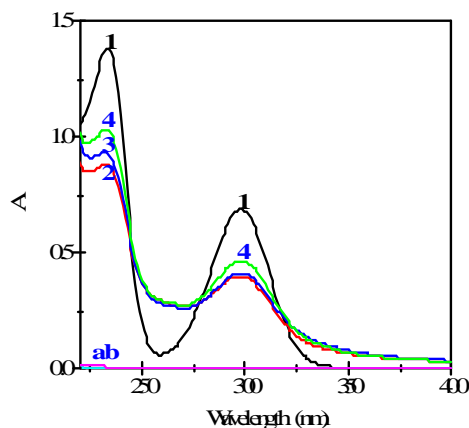


Fig. 3 The UV adsorption spectra of SA by ultrasonic-assistant electrocatalytic oxidation in the presence of mannitol with different concentration.

(Curve 1: before oxidation; after oxidation for 120 min in the presence of 0, curve 2: 1.0, curve 3 and 5.0, curve 4: $\text{mmol}\cdot\text{L}^{-1}$ mannitol.)

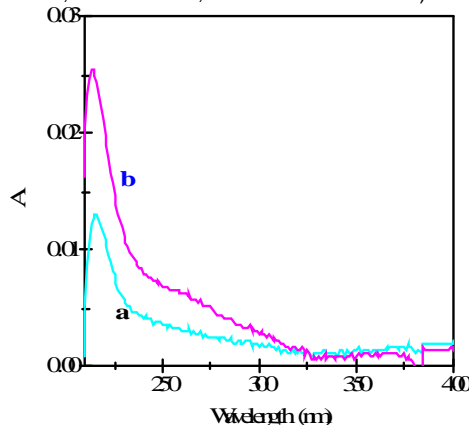


Fig. 4 The UV adsorption spectra of $5.0 \text{ mmol}\cdot\text{L}^{-1}$ mannitol before (curve a) and after (curve b) ultrasonic-assistant electrocatalytic oxidation for 60 min

According to the spectra, the presence of mannitol restrained the degradation, and the impact enhanced with the increase of mannitol concentration. So as the assistant detection, this experiment proved $\cdot\text{OH}$ was actually generated and played an important role in USECO.

2.2 UV-Vis analysis of SA degradation

2.2.1 UV-Vis spectrograms

Fig. 5 and 6 showed the pure SA ($t=0$) had two strong

absorption peaks at ≈ 235 and 298 nm, and the peak value descended as time lapsed. It proved some ultraviolet-absorbent intermediates were produced in both ECO and USECO.

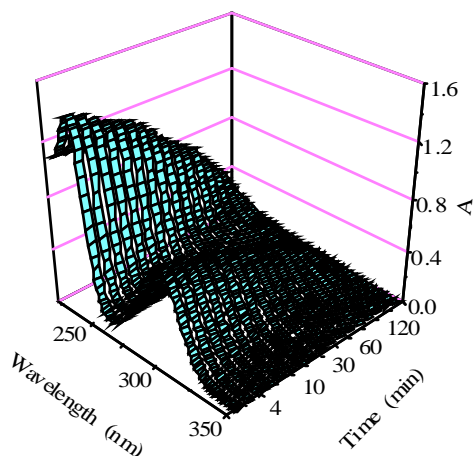


Fig. 5 UV absorption spectra in electrocatalytic oxidation of SA

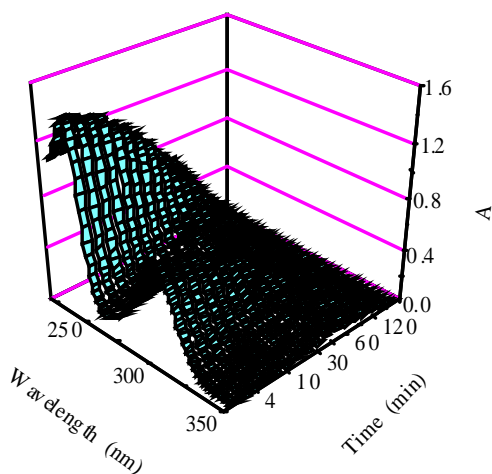


Fig. 6 UV absorption spectra in ultrasonic-assisted electrocatalytic oxidation of SA

2.2.2 Peak absorbance variation of SA (≈ 298)

The variations of relative peak absorbance of SA at ≈ 298 were presented in Fig. 7. As showed in Fig. 7, decay of relative peak absorbance in USECO met the pseudo first-order reaction kinetics, while it was more complicated in ECO. So the reduction curve was divided into two parts and fitted by NLSF separately.

The results listed in Tab.1 showed both two parts met the pseudo first-order reaction kinetics.

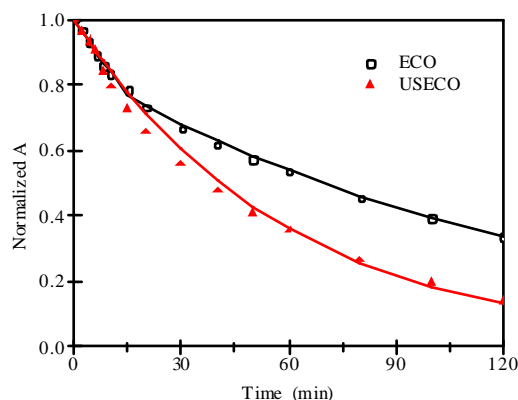


Fig. 7 Variation of peak absorbance during SA degradation

According to Tab.1, SA degradation in ECO was a process with continuous reduction of degradation rate which obeyed the pseudo first-order reaction kinetics. This phenomenon specially related to the mass transfer of reactants. As the reaction progressed, SA

Table. 1 The pseudo first-order rate constants of peak absorbance during SA degradation

process	$k_{i,SA}$ (min^{-1})
ECO	0.0171 ± 0.0007 (0-15min)
	0.0078 ± 0.0002 (15-120min)
USECO	0.0169 ± 0.0013

concentration near the electrode gradually decreased, so the diffusion from the bulk solution to the surface of electrode became the rate-determining step. Actually, during the initial period (0-15 min), degradation rates of ECO and USECO were almost identical. But after that (15-120 min), the rate constant of USECO was apparently bigger than that of ECO because ultrasonic facilitated mass transfer. The COD_{cr} variation of the sample was similar (see Tab.3).

2.3 GC-MS analysis of intermediates

The intermediates were detected by GC-MS after 60 min in USECO, and the identification and abundance were listed in Tab. 2. It was speculated that the main

Tab. 2 Identification and abundance of the intermediates fragments

Phenol		acetic acid		formic acid	
mass-to-charge ratio (m/z)	relative abundance (%)	mass-to-charge ratio (m/z)	relative abundance (%)	mass-to-charge ratio (m/z)	relative abundance (%)
95	4.0	60	70.2	46	100
94	100	46	1.4	45	32.2
74	2.5	45	90.3	44	10.3
67	2.5	44	2.8		
66	45.0	43	100		
65	32.0	42	10.2		
63	8.0	41	3.6		
62	4.0				
55	10.0				
40	12.0				
39	28.0				

intermediates were formic acid, acetic acid and phenol.

2.4 Kinetics and mechanisms of SA degradation

2.4.1 Kinetics of SA degradation

The degradation conditions were as follows: ultrasonic frequency f was 20 kHz and intensity was 27.1 W·cm⁻¹; initial pH of SA solution was 10.0; concentration of support electrolyte Na₂SO₄ C_{Na2SO4} was 10.0 g·l⁻¹; current intensity i was 5 mA·cm⁻²; temperature T was 20 °C; electrolysis time was 120 min in both ECO and USECO.

The variation curves of COD_{cr} in ECO and USECO were showed in Fig. 8.

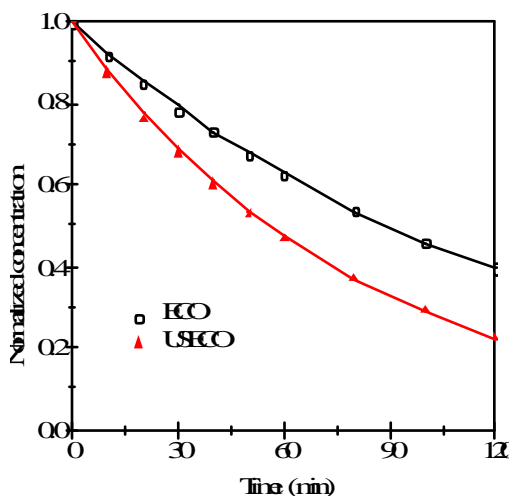


Fig. 8 COD variation of SA degradation in ECO and USECO

The COD_{cr} variations were fitted by NLSF, and the reductions in two ways both met the pseudo first-order reaction kinetics. The corresponding rate constants were listed in Tab. 3.

Tab. 3 The pseudo first-order rate constants of COD reduction during SA degradation processes

process	$k_{1, \text{COD}}$ (min ⁻¹)
ECO	0.0078±0.0002
USECO	0.0125±0.0003

Compared with degradation of phenol and benzoic acid, the rate of COD_{cr} reductions of SA in both processes obviously increased. And pseudo first-order rate constant ($k_{1, \text{COD}}$) of USECO was much bigger than that of ECO. Due to ultrasonic cavitation and sonochemical reaction, temperature, pressure and radical yield of the solution were all improved which caused the increase of SA degradation rate.

2.4.2 Mechanisms of SA Degradation

The formation of these intermediates indicated that SA was attacked by ·OH and its carboxyl was substituted by hydroxyl to create phenol which successively reacted with ·OH to generate dihydroxybenzene and trihydroxybenzene.¹¹ These intermediates were further oxidized into quinones, and then the benzene ring was cleaved to form formic acid and acetic acid, which were finally degraded into CO₂ and H₂O. Furthermore, capture of ·OH by SA in the system of xanthine and 2,6-dihydropyrimidine had been reported in 1981 by Ramsay et al.²⁹ The generation of dihydroxybenzoic acid in phosphate buffer at pH=7 proved that SA had the ability of hydroxylation. In 2001, our team adopted the same method but at pH=11 to research the capture of ·OH



- precipitation process. *Industrial Water Treatment*. 2010; 30: 31-34.
7. Chen, G. Y., Chen, H. B., He, C. B., Zhang, X. L., Qian, W. W. An study of BAF on the treatment on the simulated greywater in winter. *Chinese Journal of Environmental Science and Management*. 2008; 33: 55-58.
8. Zhang, X. L., Mei, B., Chen, G. Y., Ma, Q. Treatment of high saline wastewater by enhanced contact oxidation. *Chinese journal of Environmental Science and Technology*. 2008; 31: 153-56.
9. Chrysochoou, M., Zhang, X. & Amador, J. A. Aerobic Cr(VI) Reduction by Bacteria in Culture and Soil Conditions. *Soil Sediment Contam. An Int. J.* 2013; 22: 273-87.
10. Bhatkhande, D. S., Pangarkar, V. G. & Beenackers, A. A. Photocatalytic degradation for environmental applications - a review. *J. Chem. Technol. Biotechnol.* 2002; 77: 102-16 .
11. Scheck, C. Degradation of phenol and salicylic acid by ultraviolet radiation/hydrogen peroxide/oxygen. *Water Res.* 1995; 29: 2346-52.
12. Su, C., Hong, B.-Y. & Tseng, C.-M. Sol-gel preparation and photocatalysis of titanium dioxide. *Catal. Today*. 2004; 96: 119-26.
13. Liu, H., Liu, Y., Zhang, C. & Shen, R. Electrocatalytic oxidation of nitrophenols in aqueous solution using modified PbO₂ electrodes. *J. Appl. Electrochem.* 2007; 38: 101-08.
14. Pelegri, R., Peralta-Zamora, P., de Andrade, A. R., Reyes, J. & Durán, N. Electrochemically assisted photocatalytic degradation of reactive dyes. *Appl. Catal. B Environ.* 1999; 22: 83-90.
15. Li, X.-Y., Cui, Y.-H., Feng, Y.-J., Xie, Z.-M. & Gu, J.-D. Reaction pathways and mechanisms of the electrochemical degradation of phenol on different electrodes. *Water Res.* 2005; 39: 1972-81.
16. Li, Y., Wang, F., Zhou, G. & Ni, Y. Aniline degradation by electrocatalytic oxidation. *Chemosphere*. 2003; 53: 1229-34.
17. Nouri-Nigjeh, E., Bruins, A. P., Bischoff, R. & Permentier, H. P. Electrocatalytic oxidation of hydrogen peroxide on a platinum electrode in the imitation of oxidative drug metabolism of lidocaine. *Analyst* 2012; 137: 4698-702.
18. Chen, X. M., da Silva, D. R. & Martínez-Huitle, C. A. Application of advanced oxidation processes for removing salicylic acid from synthetic wastewaters. *Chinese Chem. Lett.* 2010; 21: 101-04.
19. Lin, S. H. & Wu, C. L. Electrochemical nitrite and ammonia removal from aqueous solution. *J. Environ. Sci. Heal. . Part A Environ. Sci. Eng. Toxicol.* 1995; 30: 1445-56.
20. Mason, T. J. Ultrasound in synthetic organic chemistry. *Chem. Soc. Rev.* 1997; 26: 443 .
21. Wang, J. et al. Detection and analysis of reactive oxygen species (ROS) generated by nano-sized TiO₂ powder under ultrasonic irradiation and application in sonocatalytic degradation of organic dyes. *Ultrason. Sonochem.* 2011; 18: 177-83.
22. Ning, P., Bart, H.-J., Jiang, Y., de Haan, A. & Tien, C. Treatment of organic pollutants in coke plant wastewater by the method of ultrasonic irradiation, catalytic oxidation and activated sludge. *Sep. Purif. Technol.* 2005; 41: 133-39.
23. Zhai, Y. et al. Effective sonocatalytic degradation



of organic dyes by using $\text{Er}^{3+}:\text{YAlO}_3/\text{TiO}_2\text{-SnO}_2$ under ultrasonic irradiation. *J. Mol. Catal. A Chem.* 2013; 366: 282-87.

24. Reisse, J. et al. Sonoelectrochemistry in aqueous electrolyte: A new type of sonoelectroreactor. *Electrochim. Acta.* 1994; 39: 37-39.

25. Mohapatra, S., Misra, M., Mahajan, V. , Raja, K. A novel method for the synthesis of titania nanotubes using sonoelectrochemical method and its application for photoelectrochemical splitting of water. *J. Catal.* 2007; 246: 362-69.

26. Compton, R. G., Eklund, J. C. & Marken, F. Sonoelectrochemical processes: A review. *Electroanalysis* 1997;9: 509-22.

27. Fockede, E. & Van Lierde, A. Coupling of anodic and cathodic reactions for phenol electro-oxidation using three-dimensional electrodes. *Water Res.* 2002; 36: 4169-75.

28. Montilla, F., Morallón, E., De Battisti, A. & Vázquez, J. L. Preparation and Characterization of Antimony-Doped Tin Dioxide Electrodes. Part 1. Electrochemical Characterization. *J. Phys. Chem. B.* 2004; 108: 5036-43.

29. Richmond, R., Halliwell, B., Chauhan, J. & Darbre, A. Superoxide-dependent formation of hydroxyl radicals: Detection of hydroxyl radicals by the hydroxylation of aromatic compounds. *Anal. Biochem.* 1981; 118: 328-35.